ISSN 1069-3513, Izvestiya, Physics of the Solid Earth, 2009, Vol. 45, No. 5, pp. 381–394. © Pleiades Publishing, Ltd., 2009.
Original Russian Text © A.A. Lyubushin, 2009, published in Fizika Zemli, 2009, No. 5, pp. 15–28.

Synchronization Trends and Rhythms of Multifractal Parameters of the Field of Low-Frequency Microseisms

A. A. Lyubushin

Schmidt Institute of Physics of the Earth, Russian Academy of Sciences,
Bol'shaya Gruzinskaya ul. 10, Moscow, 123995 Russia

Received August 1, 2008

Abstract—The field of low-frequency microseisms is investigated with the use of data from 83 stations of the F-net broadband network in Japan over the period from the beginning of 1997 through June 2008. Vertical components with a sampling step of 1 s are used for analysis, as well as signals with a sampling step of 1 min obtained from the initial data by averaging and thinning. Long-period regularities of changes in the singularity spectrum support width $\Delta\alpha$ and the generalized Hurst exponent α^* for the field of low-frequency microseisms were revealed by estimating multifractal singularity spectra in consecutive time windows 30 min long for 1-s data and 24 hour long for 1-min data. The average value of the parameter $\Delta\alpha$ for 1-s data significantly decreased before the Hokkaido earthquake of September 25, 2003 ($M = 8.3$), and was not restored subsequently to its previous level. Prior to September 2003, 1-min data on α^* variations experienced strong annual changes, which completely ceased afterwards. Both these effects are interpreted as an increase in the degree of synchronization of microseismic noise on Japan's islands after the September 25, 2003, earthquake. This hypothesis is also supported by estimates of the measures of correlation and spectral coherence between variations in the average values of $\Delta\alpha$ and α^* calculated for 1-min data inside five spatial clusters of stations from consecutive time fragments two months long. Based on the well-known statement of the theory of catastrophes that synchronization is one of the flags of an approaching catastrophe, it was suggested that the Hokkaido event could be a foreshock of an even stronger earthquake nucleating in the region of Japan's islands.

PACS numbers: 91.30.Ab

DOI: 10.1134/S1069351309050024

INTRODUCTION

Low-frequency microseismic oscillations serve as an important source of information about processes proceeding in the crust, in spite of the fact that the main energy of these oscillations is caused by processes proceeding in the atmosphere and ocean, such as variations in the atmospheric pressure and the action of oceanic waves on the coast and shelf. The relation of low-frequency microseisms having periods of 5–500 s to the intensity of oceanic waves is comprehensively investigated in [Friedrich et al., 1998; Kobayashi and Nishida, 1998; Tanimoto et al., 1998; Tanimoto and Um, 1999; Ekstrom, 2001; Tanimoto, 2001; 2005; Berger et al., 2004; Kurrle and Widmer-Schnidrig, 2006; Stehly et al., 2006; Rhie and Romanowicz, 2004; 2006]. The reverse influence of low-frequency microseisms with still longer periods (from several tens to a few hundreds of minutes) on atmospheric pressure variations due to slow wave-like deformations of the lithosphere were investigated in [Lin'kov, 1987; Lin'kov et al., 1990; Petrova et al., 2007]. Actually, the Earth's crust is a medium propagating the energy from atmospheric and oceanic processes, and since the transmitting properties of the crust depend on its state, the statistical properties of microseisms reflect changes in lithospheric properties.

This basically simple idea of the use of low-frequency microseismic oscillations for monitoring the lithosphere, nevertheless, cannot be realized in a simple way. The main difficulty consists in a strong influence of numerous uncorrelated sources on the data. These sources are often diffusely distributed over the Earth's surface. Therefore, it is impossible in this case to investigate the transmitting properties of the lithosphere by controlling input actions and responses. Additionally, the division into "a signal" and "noise," which is typical of the traditional methods used for data analysis, loses its sense, when microseismic oscillations are processed. Only tidal variations in the amplitude of microseisms, as well as the arrivals and coda from the well-known strong earthquakes, can be related to "signals." These signals have been long and traditionally used in geophysics. All other microseism variations relate to "noise."

If the terminology of orthogonal wavelet analysis is used, it will be quite sufficient to retain 1% of the maximum in module wavelet coefficients and nullify all other coefficients in order to identify the signals listed above and remove noise [Lyubushin, 2008]. Evidently, such an approach is too wasteful, and the remaining 99% of information deserve more careful study. This raises the problem of investigating the statistical prop-

erties of low-frequency microseismic noise. Spectral analysis traditionally used in the geophysical practice for investigating noise is inapplicable in this case, because noise does not contain either monochromatic components or narrow-band signals. Therefore, in this paper, we use for analysis the apparatus of multifractal singularity spectra [Feder, 1988; Mandelbrot, 1982]. This method allows the most complete description of the noise structure. To analyze geophysical time series, the estimates of singularity spectra were used in [Kantelhardt et al., 2002; Currenti et al., 2005; Ramirez-Rojas et al., 2004; Ida et al., 2005; Telesca et al., 2005; Lyubushin and Sobolev, 2006; Lyubushin, 2007; 2008].

This paper continues the cycle of works on the analysis of low-frequency microseismic oscillations and the search for new precursors of strong earthquakes on their basis [Sobolev, 2004; Sobolev et al., 2005; 2008; Sobolev and Lyubushin, 2006; 2007; Lyubushin and Sobolev, 2006; Lyubushin, 2008]. The main feature of this work is the use of long-term observations of low-frequency microseisms based on the information from 83 seismic stations of the F-net broadband network (Japan) over the period from the beginning of 1997 through June 2008. Such large data volume allowed us to investigate long-period trends of the evolution of singularity spectrum parameters averaged both over the stations of the entire network and over some subgroups of these stations.

INITIAL DATA: F-NET NETWORK

Data of the F-net broadband seismic network are freely accessible on the internet at the address: http://www.hinet.bosai.go.jp/fnet. The positions of all 83 stations of the network are shown in Fig. 1. However, when the network started to function in 1997, it had only 17 stations. Subsequently, new stations were put into operation (there were an especially large number of stations in 2001), but at the same time, some of the old stations (that had been in operation since 1997) were shut down. The data to be analyzed, i.e., vertical components with a time step of 1 s (LHZ records) contain intervals with gaps and incorrect data (such as constant zero values) due to malfunctions of measuring and recording instrumentation.

Data were loaded in the form of 2-month long time fragments. For each station, the loaded record began at 00:00:00 of the following day (month-day format): 01.01, 03.01, 0.5.01, 07.01, 09.01, and 11.01. If inside the 2-month fragment of data, the record began not from these standard initial time marks, such a record was rejected. Small gaps, no longer than 2 h, were filled in accordance with the signal behavior to the right and to the left from the gap in time intervals of the same length as the gap length. If the record contained longer gaps and malfunctions, we considered only the initial part of such a record (preceding the first long gap). Such a choice corresponds to the rules of functioning of the F-net database, according to which the user has the right to load an indefinitely large amount of information, but in the form of discrete portions, whose volume must not exceed 50 MB.

As a result, we accumulated an array of seismic records divided into 2-month time fragments from the beginning of 1997 through June 2008. Each 2-month fragment contains records from different stations that do not have long gaps and begin synchronously. However, the lengths of these records can be different, depending on the presence of large gaps and long faulty interval. Nevertheless, for almost each 2-month fragment, there existed a fairly large number of stations ensuring a complete and continuous covering of the entire fragment length by their records. Additionally, records with a time step of 1 min were formed for each 2-month fragment of the initial 1-s data through the calculation of consecutive average values over 60 samples.

PARAMETERS OF THE SINGULARITY SPECTRUM OF LOW-FREQUENCY MICROSEISMS

Below, we briefly describe the technical details of the used singularity spectrum estimates [Lyubushin and Sobolev, 2006; Lyubushin, 2007]. The elimination of scale-dependent trends by local polynomials is an important element of this estimate. Such a procedure makes it possible to get rid of some trends (in our case, tidal and temperature variations) and investigate only relatively high-frequency pulsations of a series, i.e., precisely the noise component.

Let $X(t)$ be a random process. Define the range $\mu_X(t, \delta) = \max\limits_{t \le s \le t+\delta} X(s) - \min\limits_{t \le s \le t+\delta} X(s)$ as the measure $\mu_X(t, \delta)$ of the behavior of the signal $X(t)$ in the interval $[t, t+\delta]$ and calculate the average modulus of such measures raised to the power q:

$$M(\delta, q) = M\{(\mu_X(t, \delta))^q\}. \quad (1)$$

A random process is scale-invariant, if $M(\delta, q) \sim |\delta|^{\kappa(q)}$ at $\delta \longrightarrow 0$, i.e., there exists the limit

$$\kappa(q) = \lim_{\delta \to 0} \frac{\ln M(\delta, q)}{\ln|\delta|}. \quad (2)$$

If the dependence $\kappa(q)$ is linear, $\kappa(q) = Hq$, where $H = \text{const}$, $0 < H < 1$, then the process is monofractal [Taqqu, 1988].

For calculating the function $\kappa(q)$ from a finite sampling from the time series $X(t)$, $t = 1, \ldots, N$, it is possible to apply the DFA method [Kantelhardt et al., 2002]. Let s be the number of samples associated with the varied scale δ_s: $\delta_s = s\,\Delta t$. We divide the sampling into nonoverlapping small intervals s samples in length,

$$I_k^{(s)} = \{t: 1 + (k-1)s \le t \le ks, \quad k = 1, \ldots, [N/s]\} \quad (3)$$

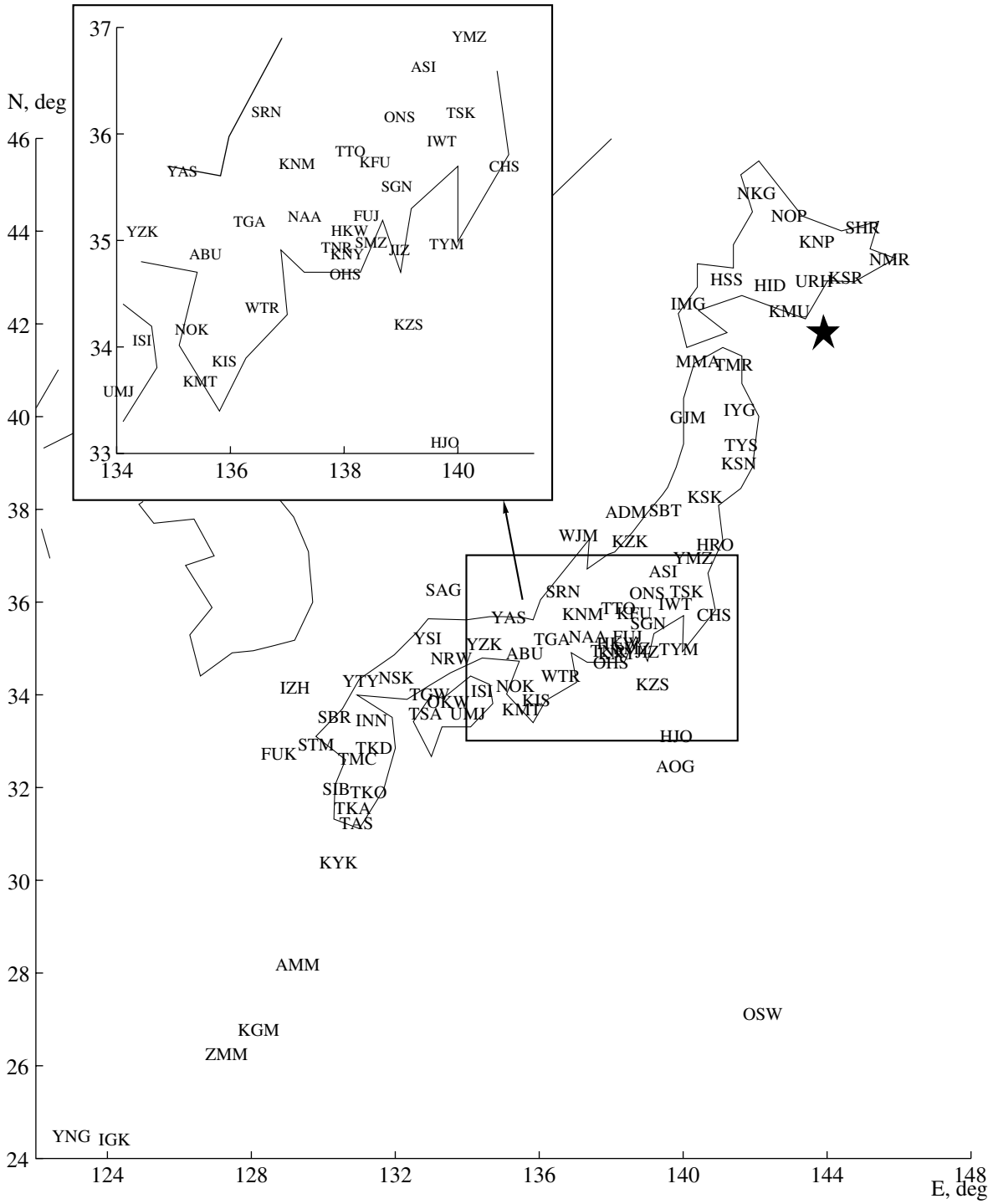

Fig. 1. Positions of 83 broadband seismic stations of the F-net network with their three-letter codes. The second letter of the code corresponds to the position of the station center. The inset in the upper left-hand corner shows the region of concentration of the stations in central Japan. The star marks the hypocenter of the September 25, 2003, earthquake (M = 8. 3) off the Hokkaido coasts.

and let

$$y_k^{(s)}(t) = X((k-1)s+1), \quad t = 1, \ldots, s \qquad (4)$$

be the part of the time series $X(t)$ corresponding to the interval $I_k^{(s)}$. Let $p_k^{(s,m)}(t)$ be a polynomial of order m fitted by the least squares method to the signal $y_k^{(s)}(t)$. Consider deviations from the local trend

$$\Delta y_k^{(s,m)}(t) = y_k^{(s)}(t) - p_k^{(s,m)}(t), \quad t = 1, \ldots, s \qquad (5)$$

and calculate the value

$$Z^{(m)}(q, s) = \left(\sum_{k=1}^{[N/s]} \left(\max_{1 \le t \le s} \Delta y_k^{(s,m)}(t) - \min_{1 \le t \le s} \Delta y_k^{(s,m)}(t) \right)^q / [N/s] \right)^{1/q}, \quad (6)$$

which will be regarded as an estimate for $(M(\delta_s, q))^{1/q}$. Now, we will define the function $h(q)$ as the coefficient of linear regression between the values $\ln(Z^{(m)}(q, s))$ and $\ln(s)$: $Z^{(m)}(q, s) \sim s^{h(q)}$. It is evident that $\kappa(q) = qh(q)$, and for a monofractal process $h(q) = H = \text{const}$.

After the determination of the function $\kappa(q)$, the next step in the multifractal analysis [Feder, 1988] is the calculation of the singularity spectrum $F(\alpha)$, which is the average fractal dimension of the time moments τ_α, which have the same value of the local Goelder–Lipshitz exponent: $\lambda(t) = \lim_{\delta \to 0} \frac{\ln(\mu(t, \delta))}{\ln(\delta)}$, i.e., $\lambda(\tau_\alpha) = \alpha$. The standard approach consists in the calculation of the Gibbs statistical sum

$$W(q, s) = \sum_{k=1}^{[N/s]} \left(\max_{1 \le t \le s} \Delta y_k^{(s,m)}(t) - \min_{1 \le t \le s} \Delta y_k^{(s,m)}(t) \right)^q \quad (7)$$

and the determination of the mass indicator $\tau(q)$ from the condition $W(q, s) \sim s^{\tau(q)}$, after which the spectrum $F(\alpha)$ is calculated by the formula

$$F(\alpha) = \max\{\min_q(\alpha q - \tau(q)), 0\}. \quad (8)$$

Comparing (6) and (7), it is easy to see that $\tau(q) = \kappa(q) - 1 = qh(q)$. Thus, $F(\alpha) = \max\{\min_q q(\alpha - h(q)) + 1, 0\}$.

If the singularity spectrum $F(\alpha)$ is estimated in a moving time window, its evolution provides information about changes in the noise structure. In particular, the position and width of the support of the spectrum $F(\alpha)$, i.e., the values $\alpha_{\min}$, $\alpha_{\max}$, $\Delta\alpha = \alpha_{\max} - \alpha_{\min}$, and α^* ($F(\alpha^*) = \max_\alpha F(\alpha)$) are the characteristics of noise. The quantity α^* is called the generalized Hurst exponent. For a monofractal signal, the value of $\Delta\alpha$ must be zero, and $\alpha^* = H$. Usually, $F(\alpha^*) = 1$, but there exist windows, for which $F(\alpha^*) < 1$. In the general case, $F(\alpha^*)$ is equal to the fractal dimension of the multifractal measure support [Feder, 1988].

In the calculation of $\Delta\alpha$ and α^*, we were guided by the following considerations. The exponent q was varied within the interval $q \in [-Q, +Q]$, where Q is a certain sufficiently large number, for example, $Q = 10$. For each value of α within the interval $\alpha \in [A_{\min}, A_{\max}]$, where $A_{\min} = \min_{q \in [-Q, +Q]} \frac{d\tau(q)}{dq}$, and $A_{\max} = \max_{q \in [-Q, +Q]} \frac{d\tau(q)}{dq}$, we calculated the value $\tilde{F}(\alpha) = \min_{q \in [-Q, +Q]} (\alpha q - \tau(q))$. If the value of α is close to $A_{\min}$, then $\tilde{F}(\alpha) < 0$, and this value is unsuitable as an estimate of the singularity spectrum, which must be non-negative. However, beginning from a certain α, the value $\tilde{F}(\alpha)$ becomes non-negative, and this condition defines the $\alpha_{\min}$ value. At a further α increase, the value $\tilde{F}(\alpha)$ increases, reaches its maximum when $\alpha = \alpha^*$, then begins to decrease, and finally, attains a certain value $\alpha_{\max} < A_{\max}$, at which $\tilde{F}(\alpha)$ again becomes negative, if $\alpha > \alpha_{\max}$. Thus, $F(\alpha) = \tilde{F}(\alpha)$ provided that $\tilde{F}(\alpha) \ge 0$, which determines the interval of the singularity spectrum support $\alpha \in [\alpha_{\min}, \alpha_{\max}]$. The derivative $\frac{d\tau(q)}{dq}$ is calculated numerically from the values $\tau(q)$, $q \in [-Q, +Q]$, and the accuracy of its calculation is of little significance, because this derivative is used for a rough determination of an a priori interval of possible exponents q.

Below, in the analysis of low-frequency microseisms, we used the estimates of singularity spectra in the following successive nonoverlapping time windows: for the initial 1-s data, in the window 30 min long (1800 samples), and for 1-min data, in the window 24 h long (1440 samples). In the first case, local trends were removed by fourth-order polynomials, and in the second case, by eighth-order polynomials. Additionally, for estimating the spectral measure of coherence between variations in the singularity spectra parameters for 1-min data, we used the moving time window 12 h long (720 samples) with the shift by 1 h (60 samples). In this case, scale-dependent trends were removed by local fourth-order polynomials.

Most of the attention will be concentrated on changes in two parameters of the singularity spectrum, namely, the generalized Hurst exponent α^* and the singularity spectrum support $\Delta\alpha$. The quantity α^* characterizes the most typical and often met Goelder–Lipshitz exponent, whereas $\Delta\alpha$ reflects the diversity of the random behavior of the signal, and, as will be discussed below, this quantity is a peculiar measure for the number of hidden degrees of freedom of a stochastic system.

VARIATIONS IN THE SINGULARITY SPECTRUM SUPPORT WIDTH

Figure 2 shows examples of the plots of estimates of the singularity spectrum $F(\alpha)$ in one of the windows for 1-s (Fig. 2a) and 1-min (Fig. 2d) data obtained at one of the stations of the network (KSK). In addition, the plots of variations in the parameters α^* and $\Delta\alpha$ during the 2-month fragment (July 1–August 31, 2006) for 1-s (Figs. 2b, 2c) and 1-min (Figs. 2e, 2f) are given below each plot $F(\alpha)$. The sharp outliers in Figs. 2b and 2c reflect the influence of arrivals from different close and remote earthquakes. These outliers are absent in Figs 2e

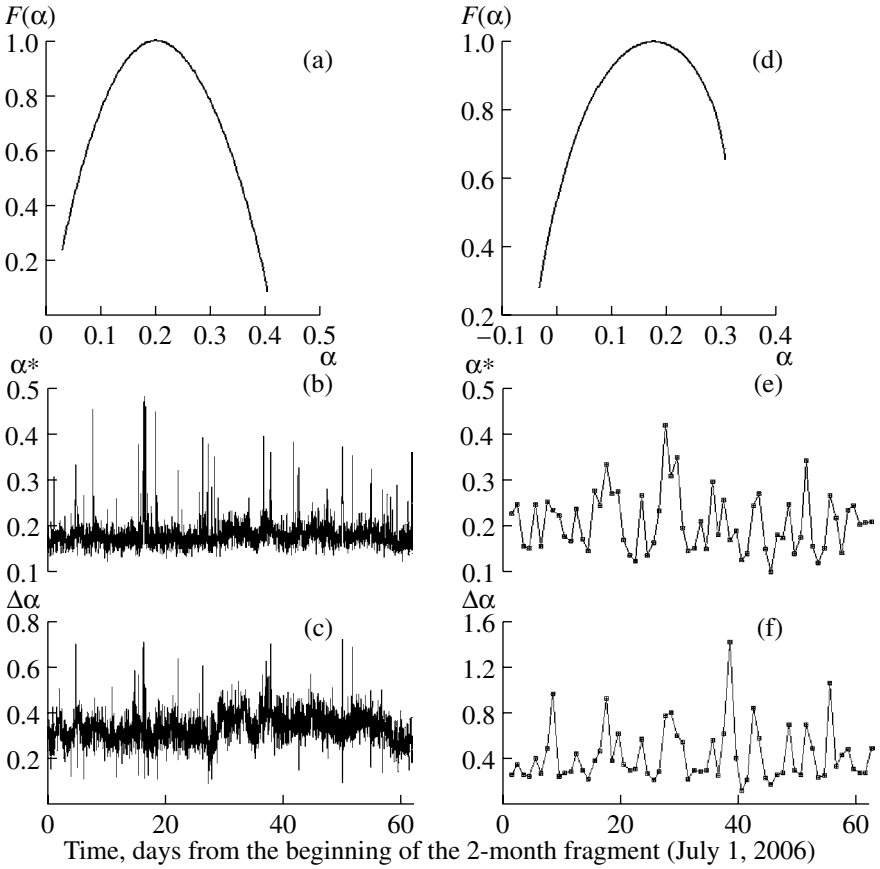

Fig. 2. Plots showing estimates for the singularity spectrum $F(\alpha)$ and variations in its parameters: the generalized Hurst exponent α^* and the singularity spectrum support width $\Delta\alpha$, at the KSK station for the 2-month fragment (July 1–August 31, 2006): (a), (b), and (c) for 1-s data in the consecutive intervals 30 min long (1800 samples); (d), (e), and (f) for 1-min data in the consecutive intervals 24 h long (1440 samples); (a) and (d) are presented for one of the intervals specified above.

and 2f due to double averaging: first, in passing from the 1 s to 1 min time step, and then in passing from the window length 30 min to the window length 24 h.

Consider the set of estimates of the parameter $\Delta\alpha$ for 1-s data (Fig. 2c). For each 30-min window, in which these estimates were obtained, there exist a certain number of stations supporting these estimates by their data. The number of such stations changes from one 2-month fragment to another and inside each fragment. We will calculate for each 30-min window the median of $\Delta\alpha$ values over all stations, whose data are suitable for analysis. The median is a robust (stable with respect to the outliers) alternative to an ordinary average value.

The sequence of medians $\Delta\alpha$ over all stations will form one continuous time series, whose total duration is 11.5 yr and the time step is 30 min. This time series is a certain integral statistical characteristic of the field of the microseism. Let us consider the behavior of this series at different types of smoothing. Gaussian trends with definite optimal properties are chosen as the method of smoothing [Hardle, 1989]. The following quantity:

$$\bar{X}(t|H) = \int_{-\infty}^{+\infty} X(t + H\xi)\psi(\xi)d\xi \Big/ \int_{-\infty}^{+\infty} \psi(\xi)d\xi, \qquad (9)$$
$$\psi(\xi) = \exp(-\xi^2),$$

will be called the Gaussian trend $\bar{X}(t|H)$ of the signal $X(t)$ with the parameter (radius) of smoothing $H > 0$.

For time series with discrete times, quantity (9) can be efficiently calculated with the use of the fast Fourier transform. This method of averaging was applied to the investigation of microseisms in [Sobolev and Lyubushin, 2006; Lyubushin, 2007]. According to formula (9), the average value roughly relates to the interval with the center at the point t with the radius H.

Two values of the radius: $H = 13$ days and $H = 0.5$ yr, were used for smoothing the $\Delta\alpha$ medians. The results of smoothing the medians over all stations are presented in Fig. 3b: the plots of smoothing with the radii 13 days and 0.5 yr are shown by the gray and bold black lines, respectively. The synchronous sequence of magnitudes ($M \geq 6$) of seismic events in the rectangular region $20° \leq 60°$ N and $120° \leq 160°$ E is presented in Fig. 3a. In this figure, the vertical gray line with the arrow indicates the

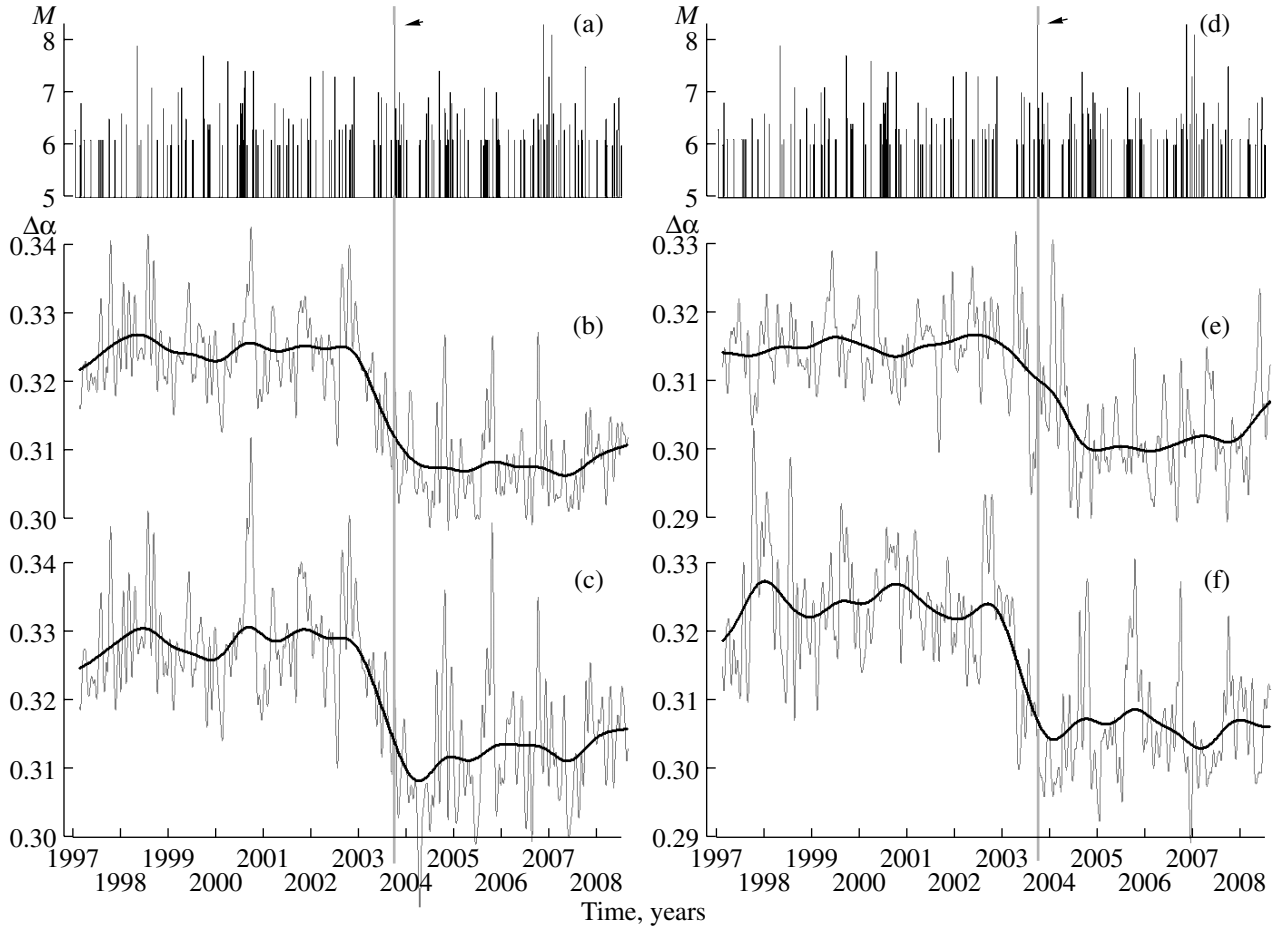

Fig. 3. (a), (d) Identical sequences of magnitudes ($M \geq 6$) of seismic events in the rectangular region between 20°–60° N and 120°–160° E; (b), (c), (e), and (f) results of the Gaussian smoothing of variations in the median of the singularity spectrum support width $\Delta\alpha$ for 1-s data in the consecutive intervals 30 min long: gray lines show the smoothing with a radius of 13 days and the bold black lines, with a radius of 0.5 yr. The median is determined (b) for all 83 stations of the network; (c) for 41 central stations (34°–39° N); (e) for 17 northern stations (≤ 39° N); and (f) for 25 southern stations (34° N). The vertical gray lines with the arrows mark the time moment of the Hokkaido earthquake of September 25, 2003 (M = 8.3).

time moment of the Hokkaido earthquake of September 25, 2003 (M = 8.3).

An important feature of the behavior of the $\Delta\alpha$ value smoothed with H = 0.5 yr (Fig. 3b) is its considerable drop, which began early in 2003, half a year before the Hokkaido event. The average level of the parameter attained after this event did not return to its previous value. Additionally, one should pay attention to a clearly pronounced annual periodicity in variations of the value smoothed with the radius H = 13 days (gray line in Fig. 3b): an outburst of this value, as a rule, falls on July–August, which is especially clearly seen in 2000, 2002, and 2004–2006.

To check the stability of the result obtained, i.e., a decrease in the average value of $\Delta\alpha$, analogous estimates were calculated for some stations of the network: for 41 central stations with latitudes from 34° to 39° N (Fig. 3c); for 17 northern stations with latitudes ≥39° N (Fig. 3e); and for 25 southern stations with latitudes ≤34° N (Fig. 3f). Figure 3d is identical to Fig. 3a and is presented here for convenience of comparing Figs. 3e and 3f with the seismic regime.

It is seen from Figs. 3c, 3e, and 3f that the average value of $\Delta\alpha$ decreases independently of the set of stations, for which it is calculated. The annual periodicity at the smoothing with the radius H = 13 days (Figs. 3b, 3f) remains nearly the same as for all stations (Fig. 3b). Note also that after the Hokkaido earthquake, annual variations in $\Delta\alpha$ (Figs. 3b, 3c, 3f) became more clearly pronounced, whereas the annual periodicity is pronounced less clearly for the northern stations.

VARIATIONS IN THE GENERALIZED HURST EXPONENT

We will now consider the median of estimates for the generalized Hurst exponent α^* obtained from different stations for 1-min data (Fig. 2e). The median is

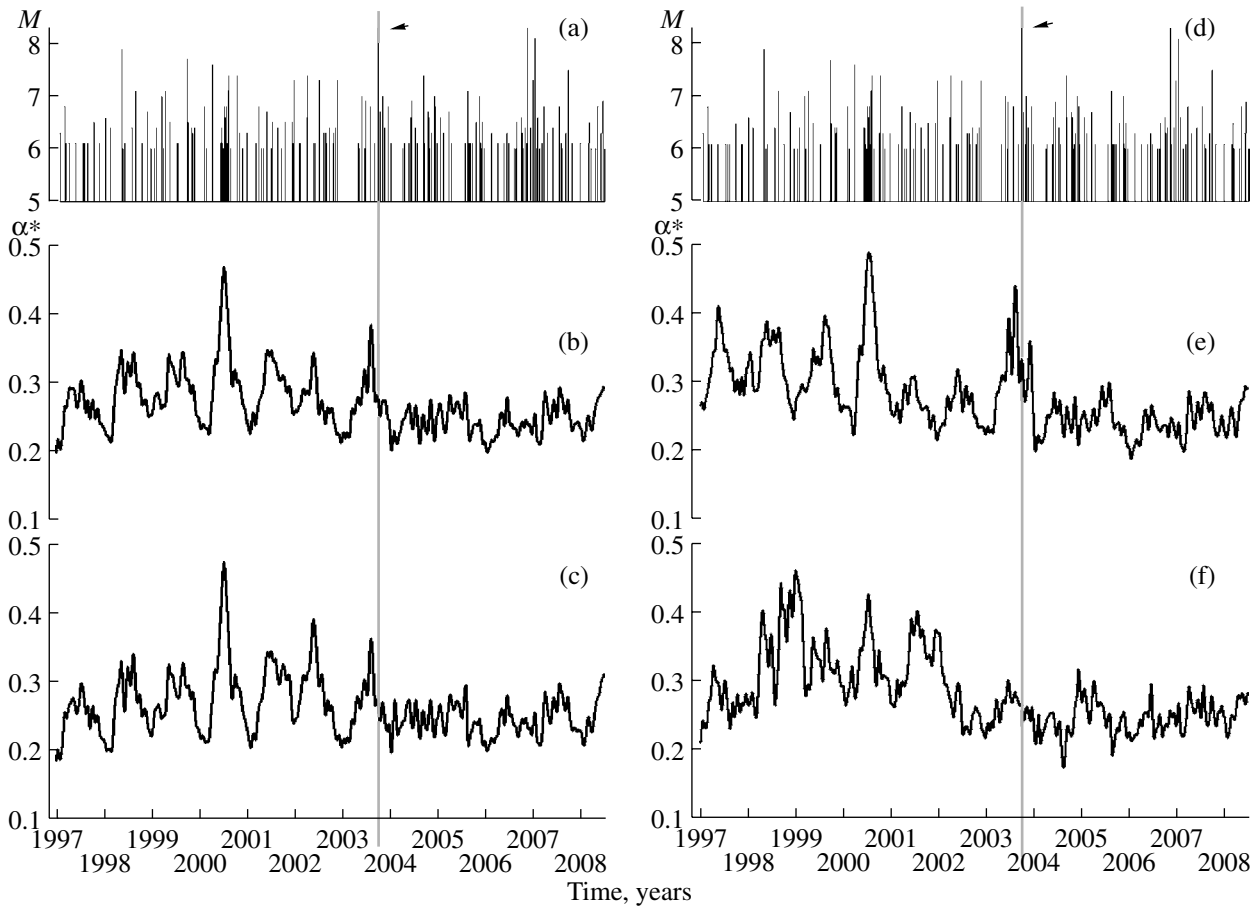

Fig. 4. (a), (d) Identical sequences of magnitudes ($M \geq 6$) of seismic events in the rectangular region between 20°–60° N and 120°–160° E; (b), (c), (e), and (f) results of the Gaussian smoothing of variations in the median of the generalized Hurst exponent α* for 1-min data in the consecutive intervals 24 h long with the radius of smoothing 13 days. The median is determined (b) for all 83 stations of the network; (c) for 41 central stations (34°–39° N); (e) for 17 northern stations (≤ 39°N); and (f) for 25 southern stations (34° ≤ N). The vertical gray lines with the arrows mark the time moment of the Hokkaido earthquake of September 25, 2003, ($M = 8.3$).

calculated by the same method as in the preceding section, but instead of the 30-min window, the 24-h window (1440 minute samples) is used. As a result, we obtain the time series of the α* medians, whose duration is 11.5 yr and the time step is 24 h. This series is smoothed according to formula (9) with the radius $H =$ 13 days. The result is presented in Fig. 4. Just as in Fig. 3, Figs. 4a and 4d are also identical to each other and depict the sequence of magnitudes of strong events in the rectangular vicinity of Japan islands. Figures 4b, 4c, 4d, and 4f show the plots of smoothed values of the α* median calculated, respectively, for all 83 stations of the network, consisting of 41 central stations, 17 northern stations, and 25 southern stations.

The main feature of the plots presented in Fig. 4 is the behavior of the seasonal component of the variations. This component is clearly pronounced before the Hokkaido event (to a lesser degree for the southern stations (Fig. 4f)) but decreases afterwards.

VARIATIONS IN THE PRODUCTS OF CLUSTER CANONICAL CORRELATIONS

This and the next sections of the paper will be devoted to the investigation of measures of correlation and coherence between variations in both the support width Δα and the generalized Hurst exponent α* estimated for 1-min data for different parts of the network. The choice of 1-min data for this purpose was dictated by the circumstance that, based on experience, the lower the frequency of the variations in singularity spectrum parameters, the greater the amount of coherence effects that are observed in them. The main correlations and coherences during the investigation of 1-s data are caused by a trivial presence of traces of arrivals from large and moderate earthquakes, which is of weak interest.

In our case, it is necessary to construct statistics that would more or less objectively reflect an increase or a decrease in the total correlation or coherence of the behavior of singularity spectrum parameters during the

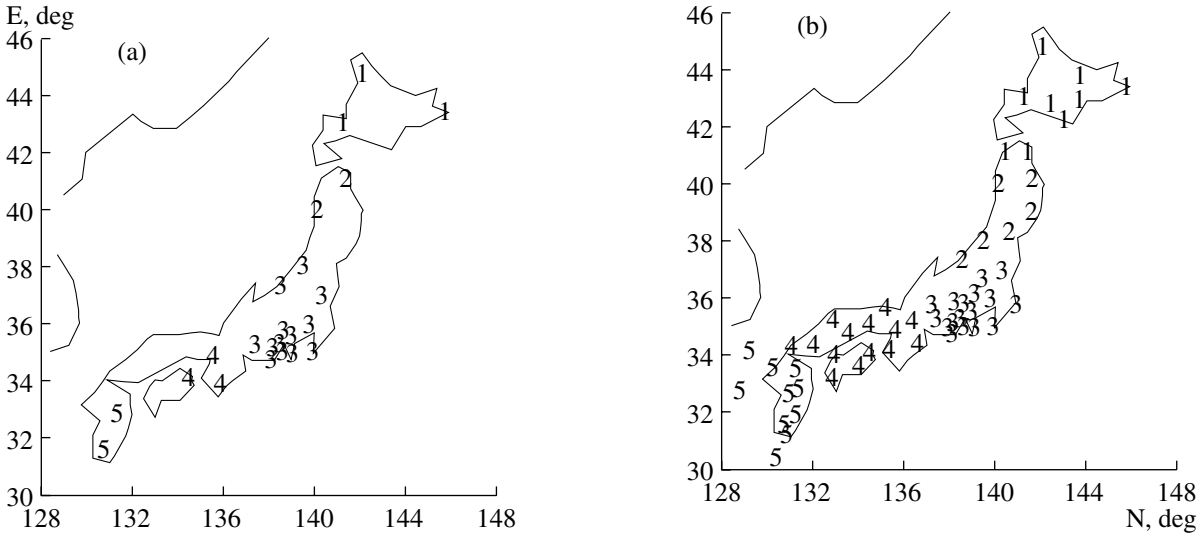

Fig. 5. Examples of the division of stations, according to their positions, into five clusters for two 2-month fragments: (a) for the fragment September 1–October 31, 1998, 23 stations; and (b) for the fragment July 1–August 31, 2002, 57 stations. The stations belonging to the same cluster have identical numbers.

entire interval of observations (1997–2008), in spite of the fact that some stations ceased operations long before the end of the analyzed time interval, and some stations started to operate after its beginning. In addition, due to malfunctions of the instrumentation and recording systems, data from some or other station can be absent in the 2-month fragment under consideration, in spite of their presence in the preceding and subsequent fragments. The fragmentary character of the data from any station is a substantial methodological barrier for a direct application of multidimensional spectral coherence measures [Lyubushin, 1998; 2007; 2008; Lyubushin and Sobolev, 2006; Sobolev and Lyubushin, 2007] to the analysis of relations between the readings of different stations, because the synchronism and continuity of data are required for calculating the statistics of coherence.

However, the presence of a large number of stations allows us to overcome this difficulty by considering *cluster measures* of the multidimensional correlation and coherence. The essence of this approach is as follows: only the stations, which possess continuously recorded data throughout the entire 2-month fragment, are considered. Further, these stations are grouped to always form the same number of spatial clusters. Below, the number of clusters was assumed to be five, i.e., all stations with continuous records during the 2-month fragment under consideration are always divided into five clusters in accordance with the spatial positions of the stations. The number of clusters (5) was chosen, because this number is not too large but sufficiently large for a more or less uniform covering of the seismically active territory under consideration (Japan's islands). The use of the same number of clusters for all 2-month fragments eliminates the influence of dimensionality on the values of the measures of correlation or coherence and allows their comparison with each other, regardless of the number of suitable stations in some or other 2-month fragment.

Figure 5 shows two examples of the automatic division of the network stations with continuous records for 2-month fragments into five clusters. The stations belonging to the same spatial cluster are designated by the same numeral (cluster number). Stations were automatically divided into five clusters by using the method of hierarchical clusterization with the "far neighbor" metric [Duda and Hart, 1973]. The use of this metric instead of the often used "nearest neighbor" metric makes it possible to obtain compact "rounded" clusters and avoid long "chain-like" clusters. The characteristic linear scale of the clusters obtained varied from 120 to 350 km.

When cluster measures are considered, solitary stations must be excluded from the analysis, because during the automatic division, they will always form individual clusters consisting of one element. In our case, there were six such stations located on the remote islands, and they could be excluded from the analysis through restricting the stations' latitude to not less than 30° N (Fig. 1).

After the division of stations into clusters, we calculated the average values of the parameters $\Delta\alpha$ and α^* in each time window (equal in this case to 24 h) for the stations included in the same cluster. Thus, independently of the number of suitable stations in the 2-month fragment, after the clusterization, we always obtained two 5-dimensional time series of variations in the average cluster values of $\Delta\alpha$ and α^*. Such a method makes it possible, on the one hand, to take into account the contributions of stations located in different subregions of a seismically active region and, on the other hand, to compensate for the fragmentary character of data caused by instrumental malfunctions.

We should stress once more that both the positions of the cluster centers and the number of stations in each cluster vary, as a rule, from one 2-month fragment to another. Only two factors remain unchanged: (1) the number of the output average values of $\Delta\alpha$ and α^* is always equal to five, and (2) the clusters more or less uniformly cover the territory under investigation. These circumstances allow us to consider the multidimensional measures of the correlation or coherence between the components of the obtained 5-dimensional time series as an integral measure reflecting the general correlation of changes in the multifractal characteristics of the field of low-frequency microseismic noise.

In order to obtain a multidimensional measure of the correlation of the average values of $\Delta\alpha$ or α^* corresponding to a chosen 2-month fragment, we will use the Hotelling construction of canonical correlations [Hotelling, 1936; Rao, 1965]. Let $x_j(t)$, $j = 1, \ldots, m$ be an m-dimensional time series, and $t = 1, \ldots, N$ be discrete time. In our case, $m = 5$, x_j are the average cluster values of $\Delta\alpha$ or α^*, and t is the index numbering the consecutive days inside the 2-month fragment. Let us select the component with the number k and consider the regression model of the influence of all the other components on the selected component x_k

$$\begin{aligned} x_k(t) &= y_k(t) + \varepsilon_k(t), \\ y_k(t) &= \sum_{j=1,\, j\neq k}^{m} \gamma_j^{(k)} x_j^{(t)}. \end{aligned} \tag{10}$$

The regression coefficients $\gamma_j^{(k)}$ will be found from the condition of the minimum of the sum of squared remainders $\sum_{t=1}^{N} \varepsilon_k^2(t)$ or the sum of moduli (robust variant) $\sum_{t=1}^{N} |\varepsilon_k(t)|$. After that, we will calculate the correlation coefficient μ_k between the selected component $x_k(t)$ and the obtained regression contribution $y_k(t)$. The quantity μ_k is the canonical correlation of the kth component with respect to all other components. We perform these calculations successively for all $k = 1, \ldots, m$ and then determine the quantity

$$\kappa = \prod_{k=1}^{m} |\mu_k|. \tag{11}$$

It is obvious that $0 \le \kappa \le 1$ and the closer quantity (11) is to unity, the stronger the mutual relation of the variations in the components of the multidimensional time series $x_j(t)$ to each other. Having calculated quantities (11) for the average cluster values of $\Delta\alpha$ and α^* for all 2-month fragments, we will obtain the two sequences $\kappa_{\Delta\alpha}(\xi)$ and $\kappa_{\alpha^*}(\xi)$, where ξ is the time mark corresponding to the end of the 2-month fragment. The plots of these values are presented in Fig. 6 (thin lines with circles).

It is seen from these plots that, in spite of considerable fluctuations, the measure of correlation generally rises for both $\Delta\alpha$ and α^*. Let us smooth the dependences $\kappa_{\Delta\alpha}(\xi)$ and $\kappa_{\alpha^*}(\xi)$ by the Gaussian core according to formula (9) with the radius of averaging $H = 0.5$ yr. The results of the calculation of the Gaussian trends are presented in Fig. 6 as bold lines. A general tendency toward an increase in the measures of correlation after 2003 is seen. After the Hokkaido earthquake, the average values of correlation measures did not return to their level before 2003. Consequently, it can be inferred that the 2003 earthquake led to a prolonged increase in the average correlation of the fluctuations of the multifractal parameters of the field of low-frequency microseismic noise.

VARIATIONS IN THE CLUSTER SPECTRAL MEASURE OF COHERENCE

The measure of correlation (11) relates to the entire 2-month fragment under consideration and does not discriminate between variation frequencies. At the same time, the decomposition of this measure over different frequency bands and the stability of the correlation inside a 2-month fragment are of interest. To answer these questions, it is necessary to replace the product of the canonical correlations (11) by the spectral measure of coherence proposed in [Lyubushin, 1998], which was used, among other purposes, for the analysis of low-frequency microseisms [Lyubushin and Sobolev, 2006; Sobolev and Lyubushin, 2007; Sobolev et al., 2008; Lyubushin, 2008]. Numerous examples of the application of this measure not only in the physics of the solid Earth, but also in hydrology, meteorology, and climatic investigations are presented in [Lyubushin, 2007]. The same work contains all technical details of the calculations, which are omitted here.

The spectral measure of coherence $\lambda(\tau, \omega)$ is constructed as the module of the product of component-by-component canonical coherences

$$\lambda(\tau, \omega) = \prod_{j=1}^{m} |\nu_j(\tau, \omega)|. \tag{12}$$

Here, $m \ge 2$ is the total number of jointly analyzed time series; ω is frequency; τ is the time coordinate of the right-hand end of the moving time window consisting of a definite number of neighboring samples; and $\nu_j(\tau, \omega)$ is the canonical coherence of the jth scalar time series, which describes the force of coupling of this series with all other series. The quantity $|\nu_j(\tau, \omega)|^2$ is the generalization of the ordinary squared spectrum of coherence between two signals for the case, when the second signal is not scalar but vector. The inequality $0 \le |\nu_j(\tau, \omega)| \le 1$ is fulfilled, and the closer the value of $|\nu_j(\tau, \omega)|$ to unity, the stronger the linear relation of variations at the frequency ω in the time window with the coordinate τ of the jth series to analogous variations in all other series. Accordingly, the quantity $0 \le \lambda(\tau, \omega) \le 1$, due to its construction, describes the effect of the cumulative coherent (synchronous, collective) behavior of all signals. Note that due to the construction of the quantity $\lambda(\tau, \omega)$, its values belong to the interval [0,1], and the

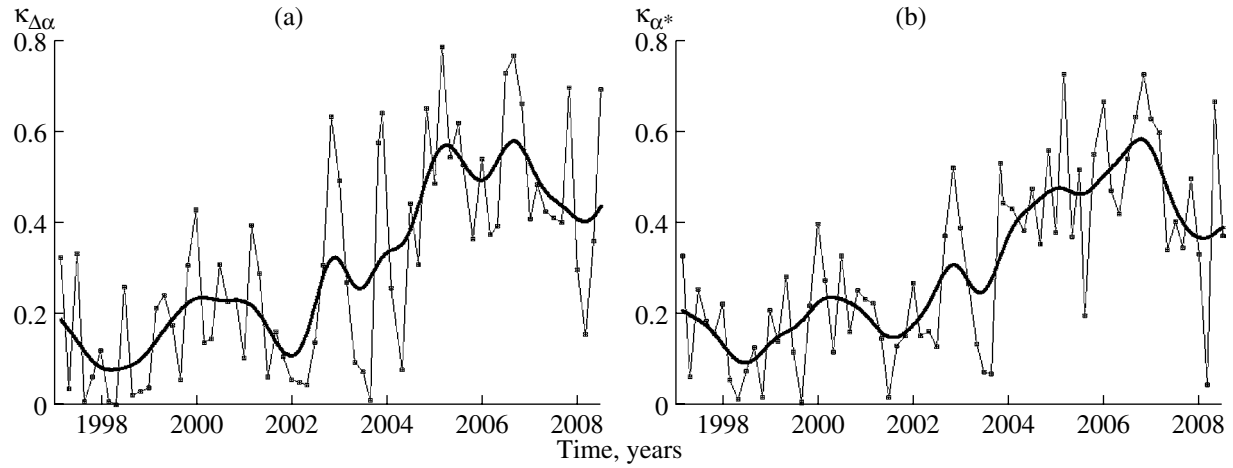

Fig. 6. Plots of variations in the product of moduli of canonical correlations (a) $\kappa_{\Delta\alpha}$ and (b) $\kappa_{\alpha*}$ between the average values of the singularity spectrum support width $\Delta\alpha$ and the generalized Hurst exponent $\alpha*$ calculated inside five spatial clusters of stations for 2-month fragments. The singularity spectra were calculated for 1-min data in the consecutive time intervals 24 h long. The bold lines are results of the Gaussian smoothing with the radius of averaging 0.5 yr.

closer the corresponding value to unity, the stronger the relation between variations in the components of the multidimensional time series at the frequency ω for the time window with the coordinate τ. It should be emphasized that the comparison of absolute values of the statistics $\lambda(\tau, \omega)$ is possible only for the same number m of simultaneously processed time series, because, due to formula (12), if m increases, λ decreases as the product of m values smaller than unity. In our case, stations are clusterized at a fixed number of clusters (5).

Since the spectral measure (12) was used for the analysis of the variability of the cumulative coherence inside 2-month fragments, singularity spectra were estimated for 1-min data in the moving time window 12 h long (720 samples) with a shift of 1 h (60 samples). Further, we again calculated the average cluster values of $\Delta\alpha$ and $\alpha*$, which thus formed five time series with a time step of 1 h (shift of the moving time window).

Below, we present the results of the application of the spectral measure (12) for the analysis of effects of the coherent behavior between the time series of variations in the average cluster values of $\alpha*$. The results for the support width $\Delta\alpha$ of the singularity spectrum are qualitatively analogous. To realize this method, it is necessary to have an estimate of the spectral matrix of the initial multidimensional series in each time window. Below, we prefer to use the model of vector autoregression [Marple (Jr.), 1987] of the 3rd order. To obtain the dependence $\lambda(\tau, \omega)$, the time window length was assumed to be 5 days. Since each value of $\alpha*$ was obtained in the time window 12 h long, and the shift of these windows was 1 h, the time window length for estimating the spectral matrix will be 109 samples, because $(109 - 1) \times 1 + 12 = 120$ h = 5 days.

Six frequency–time diagrams of statistics (12) for different 2-month fragments are presented in Fig. 7. These diagrams are constructed on the same scale (unified tone scale is shown on the right), depending on the position of the right-hand end of the moving time window 5 days long (time is indicated in hours from the beginning of the corresponding 2-month fragment). The sequences of magnitudes of the earthquakes with $M \geq 5$, which occurred in the rectangular vicinity of Japan's islands during the corresponding 2-month fragment, are shown above each frequency–time diagram. The 2-month fragment presented in Fig. 7d corresponds to the 2003 Hokkaido earthquake. A moderate coherence observed before the earthquake, was previously noted in [Sobolev et al., 2008; Lyubushin, 2008] from data of the IRIS broadband network. However, it should be noted that postseismic outbursts of the coherence are stronger than the precursory ones.

In addition, the outbursts of statistics (12), which can hardly be related to the postseismic or precursory coherence from some event, are seen in the frequency–time diagrams of Fig. 7 in comparison with the seismic regimes. Such coherence outbursts were noted in the work [Lyubushin, 2008], where the author suggested that a simple hypothesis stating that the coherence of the variations in parameters of the singularity spectrum of noise should be expected to increase before a strong earthquake is groundless. Indeed, meteorological or oceanic factors, including oceanic waves in very remote regions, equally can be coherence sources. The idea to investigate some scenarios of the behavior of outbursts of synchronization seems more promising [Lyubushin, 2003]. The trend of increasing the average measure of correlation presented in Fig. 6 is one such scenario. The use of spectral statistics (12) allows us to find out whether such trends are present in different frequency bands.

The values of statistics (12) for the sequence of 2-month fragments after its averaging over frequencies from certain frequency bands are presented in Fig. 8.

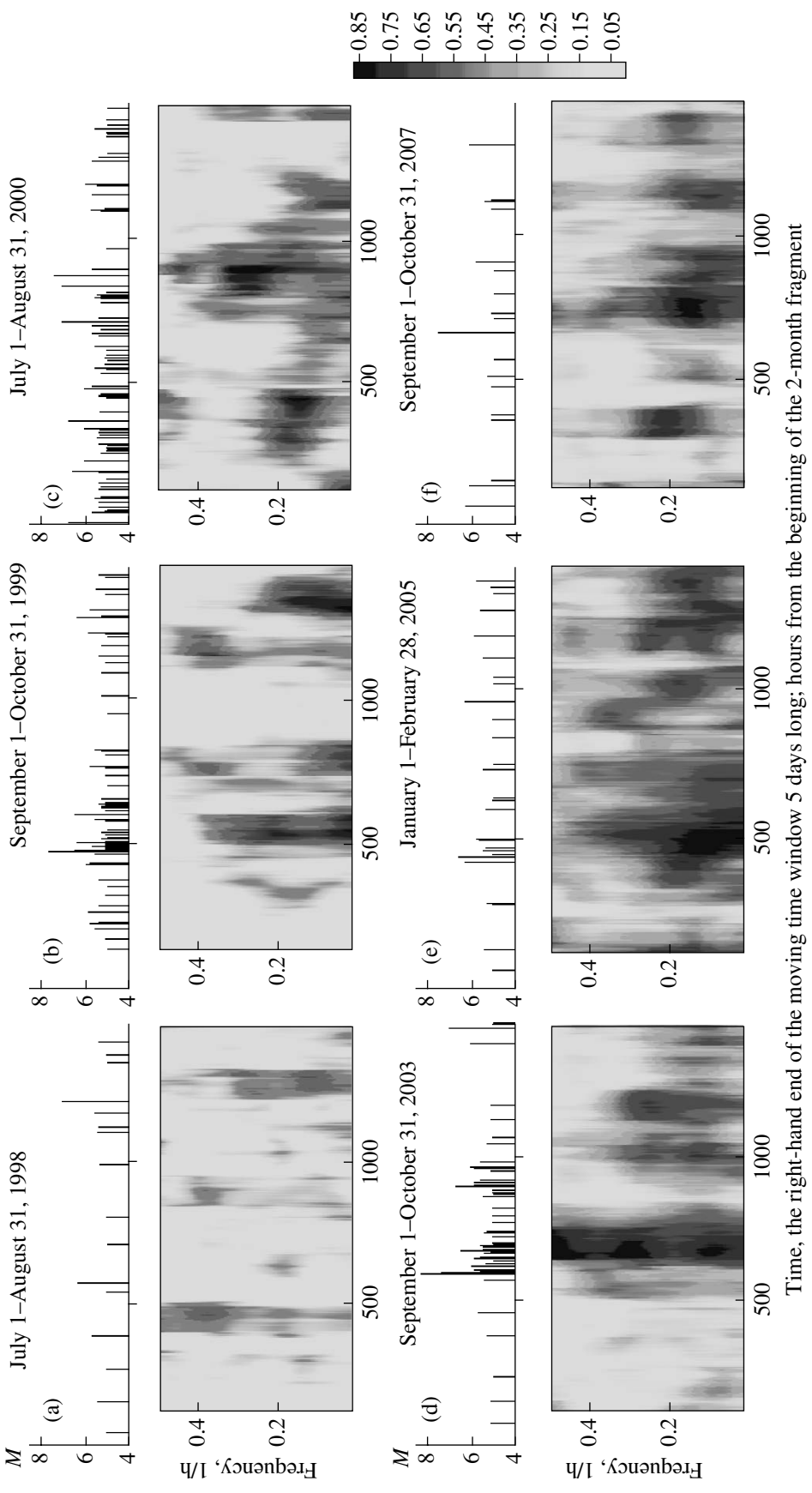

Fig. 7. Frequency–time diagrams of the evolution of the spectral measure of coherence between the average values of the generalized Hurst exponent α^*calculated inside five spatial clusters of stations for six different 2-month fragments. The measure of coherence was estimated in the moving time window 5 days long. The singularity spectra were calculated for 1-min data in the consecutive time intervals 12 h long with a shift of 1 h. The sequence of magnitudes ($M \geq 5$) of seismic events in the rectangular region between 20°–60° N an 120°–160° E is presented above each frequency–time diagram.

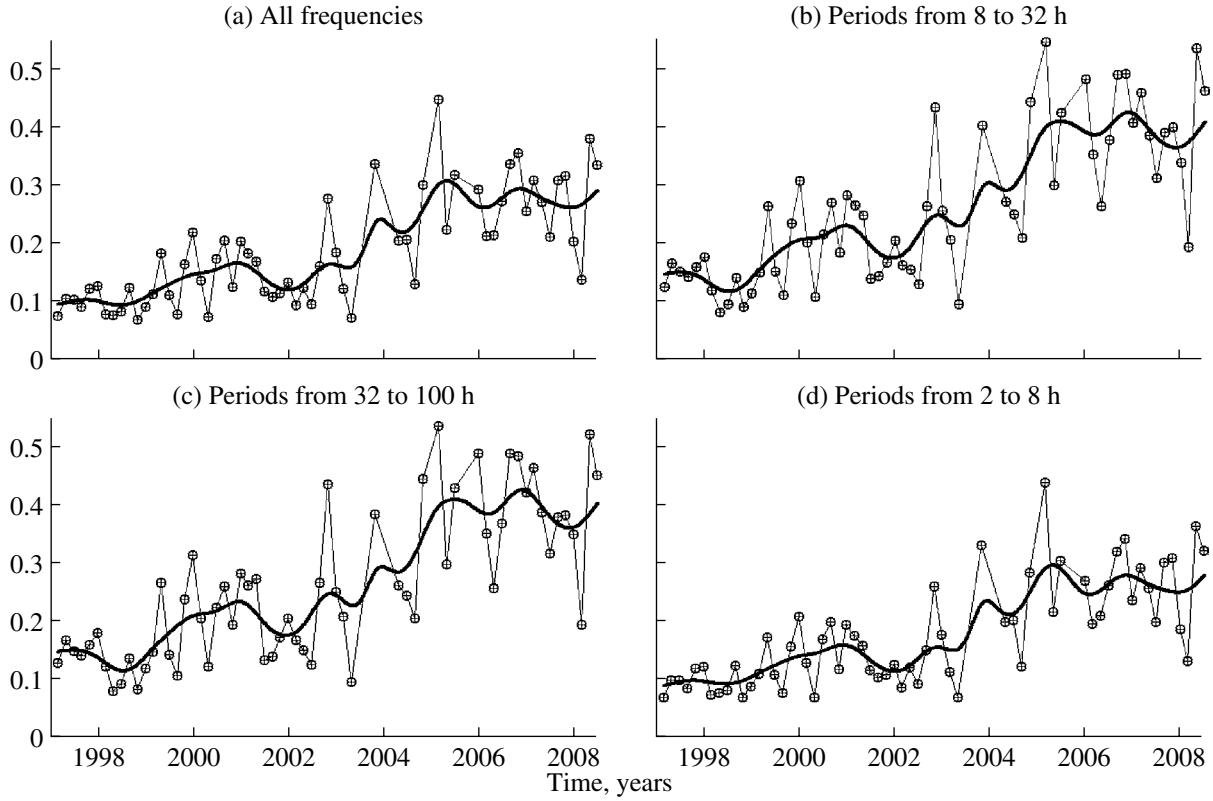

Fig. 8. Thin lines with circles are the plots of the spectral measure of coherence between the average cluster values of α^* for the consecutive 2-month fragments averaged over four different frequency bands restricted by their boundary periods (h). The bold lines are results of the Gaussian smoothing with the radius of averaging 0.5 yr. The singularity spectra were calculated for 1-min data in the consecutive time intervals 12 h long with a shift of 1 h.

Figure 8a corresponds to all frequencies; Fig. 8b, to the band with boundary periods from 8 to 32 h (containing tidal harmonics); Fig. 8c, to the low-frequency band with boundary periods of 32 and 100 h; and Fig. 8d, to the high-frequency band with boundary periods of 2 and 8 h. The Gaussian trends with a radius of averaging of 0.5 yr are shown by the bold lines. It is seen that spectral measure (12), as well as the simple measure of correlation (11), yields qualitatively the same results for all frequency bands. The average coherence increases after 2003.

Thus, changes in the state of the lithosphere after the Hokkaido earthquake of September 25, 2003, have resulted in a more correlated behavior of the multifractal characteristics of the field of microseismic noise in response to actions on the Earth's crust, which was also observed previously, in the period from 1997–2003.

DISCUSSION AND CONCLUSIONS

The analysis showed that after the Hokkaido earthquake of September 25, 2003 ($M = 8.3$), a considerable synchronization of the variations in the multifractal parameters of the low-frequency microseismic field took place and is retained to the present day. Thus, the 2003 Hokkaido earthquake, in its own way, is a crucial point in the behavior of microseisms, and this fact may testify in favor of the hypothesis that this event can be a foreshock of a still stronger earthquake.

The results presented in Figs. 3 and 4, even more clearly than the plots showing the behavior of the average measures of correlation and coherence in Figs. 6 and 8, indicate that the September 25, 2003 event is a kind of time marker separating the behavior of the field of microseisms into two modes. Additionally, Fig. 3 estimates the time of preparation of this event at 0.5 yr. The question arises as to how a decrease in the average value of $\Delta\alpha$ is related to an increase in the linear correlations between fluctuations of singularity spectrum parameters. In this sense, the quantity $\Delta\alpha$ reflects the degree of diversity of the random behavior of the signal, and therefore, its decrease is an indirect indicator of the suppression (decrease) of certain degrees of freedom of the medium.

At the same time, it is possible to find more direct analogies with a decrease in the number of degrees of freedom reflecting in the $\Delta\alpha$ decrease. Singularity spectra for the sequence of recurrence times in the Poincare cross section for systems of two coupled oscillators (Ressler and Lorenz oscillators) were numerically investigated in the works of [Pavlov et al., 2003; Ziganshin and Pavlov, 1005]. In the presence of a sufficiently

strong coupling, these oscillators become synchronous. It turned out that the synchronization of oscillators substantially decreases the singularity spectrum support width $\Delta\alpha$. Consequently, the set of results presented as plots in Figs. 3, 6, and 8 indicate that the field of microseismic oscillations in Japan after the 2003 event became synchronous, and this state is retained to the present day.

Based on the well-known statement of the theory of catastrophes that synchronization is one of the flags of an approaching catastrophe [Gilmore, 1981], it may be suggested that the Hokkaido event, notwithstanding its power (M = 8.3), could be only a foreshock of a still stronger earthquake forming in the region of Japan's islands.

As for the sharp decrease in seasonal variations of the parameter α^* for 1-min data after the September 25, 2003, earthquake, the interpretation of this result is not so transparent as for $\Delta\alpha$. We can only suggest that this decrease also reflects a blocking of some degrees of freedom of the medium, which were previously responsible for annual changes in the state of the lithosphere. On the other hand, the situation for 1-s data on $\Delta\alpha$ is the opposite: after the September 25, 2003, event, the annual variations became more clearly pronounced.

ACKNOWLEDGMENTS

I am grateful to Dr. Furumura Takashi (Earthquake Research Institute, University of Tokyo) for attracting my attention to the F-net database.

This work was supported by the Presidium of the Russian Academy of Sciences (program "The Electronic Earth"), the INTAS Foundation (project no. 05-100008-7889), and the Russian Foundation for Basic Research (project no. 06-05-64625).

REFERENCES

1. E. M. Lin'kov, *Seismic Phenomena* (LGU, Leningrad, 1987) [in Russian].
2. E. M. Lin'kov, L. N. Petrova, and K. S. Osipov, "Seismogravitational Pulsations of the Earth and Disturbances of the Atmosphere as Possible Precursors of Strong Earthquakes," Dokl. Akad. Nauk SSSR **313**(5), 1095–1098 (1990).
3. A. A. Lyubushin, "Analysis of Canonical Coherences in the Problem of Geophysical Monitoring," Fiz. Zemli, No. 1, 59–66 (1998) [Izvestiya, Phys. Solid Earth **34**, 52–58 (1998)].
4. A. A. Lyubushin, "Outbursts and Scenariosof Synchronization in Geophysical Observations," in *Sketches of Geophysical Investigations. To the 75th Anniversary of the Schmidt United Institute of Physics of the Earth* (OIFZ RAN, Moscow, 2003) pp. 130–134 [in Russian].
5. A. A. Lyubushin and G. A. Sobolev, "Multifractal Measures of Synchronization of Microseismic Oscillations in a Minute Range of Periods," Fiz. Zemli, No. 9, 18–28 (2006) [Izvestiya, Phys. Solid Earth **42**, 734–744 (2006)].
6. A. A. Lyubushin, *Analysis of Data of Geophysical and Ecological Monitoring* (Nauka, Moscow, 2007) [in Russian].
7. A. A. Lyubushin, "Microseismic Noise in a Minute Range of Periods: Properties and Possible Prognostic Indicators," Fiz. Zemli, No. 4, 17–34 (2008) [Izvestiya, Phys. Solid Earth **43** (2008)].
8. L. N. Petrova, "Seismogravitational Oscillationsof the Earth from Observations by Spaced Vertical Pendulums in Eurasia," Fiz. Zemli, No. 4, 83–95 (2002) [Izvestiya, Phys. Solid Earth **38,** 325–336 (2002)].
9. L. N. Petrova, E. G. Orlov, and V. V. Karpinskii, "On the Dynamics and Structure of Earth's Oscillations in December 2004 from Seismic Gravimeter Observations in St. Petersburg," Fiz. Zemli, No. 2, 12–20 (2007) [Izvestiya, Phys. Solid Earth **43,** 111–118 (2007)].
10. G. A. Sobolev, "Microseismic Variations Prior to a Strong Earthquake," Fiz. Zemli, No. 6, 3–13 (2004) [Izvestiya, Phys. Solid Earth **40,** 455–464 (2004)].
11. G. A. Sobolev, A. A. Lyubushin, and N. A. Zakrzhevskaya, "Synchronization of Microseismic Variations within a minute Range of Periods," Fiz. Zemli, No. 8, 3–27 (2005) [Izvestiya, Phys. Solid Earth **42**, 599–621 (2005)].
12. G. A. Sobolev and A. A. Lyubushin, "Microseismic Impulses As Earthquake Precursors," Fiz. Zemli, No. 9, 5–17 (2006) [Izvestiya, Phys. Solid Earth **42**, 721–733 (2006)].
13. G. A. Sobolev and A. A. Lyubushin, "Microseismic Anomalies before the Sumatra Earthquake of December 26, 2004," Fiz. Zemli, No. 5, 3–16 (2007) [Izvestiya, Phys. Solid Earth **43**, 341–353 (2007)].
14. G. A. Sobolev, A. A. Lyubushin, and N. A. Zakrzhevskaya, "Asymmetric Impulses, Periodicities and Synchronization of Low-Frequency Microseisms," Vulkanol. Seismol., No. 2, 135–152 (2008).
15. G. A. Sobolev, "Series of Asymmetric Impulses in a Minute Range of Microseisms As Indicators of a Metastable State of Seismically Active Zones," Fiz. Zemli, No. 4, 3–16 (2008) [Izvestiya, Phys. Solid Earth (2008)].
16. G. Currenti, C. del Negro, V. Lapenna, and L. Telesca, "Microfractality in Local Geodynamic Fields at Etna Volcano, Sisily (Southern Italy)," Natural Hazards and Earth System Sciences **5**, 555–559 (2005).
17. R. O. Duda and P. E. Hart, *Pattern Classification and Scene Analysis* (John Wiley and Sons, New York, London, Sydney, 1973; Mir, Moscow, 1976).
18. G. Ekstrom, "Time Domain Analysis of Earth's Long-Period Seismic Radiation," J. Geophys. res. **106**, N B11, 26483–26493 (2001).
19. J. Feder, *Fractals* (Plenum Press, New York, 1988; Mir, Moscow, 1991).
20. A. Friederich, F. Krüder, and K. Klinge, "Ocean-Generated Microseismic Noise Located with the Gräfenberg Array," Journal of Seismology **2**, No. 1, 47–64 (1998).
21. R. Gilmore, *Catastrophe Theory for Scientists and Engineers* (John Wiley and Sons, New York, 1981; Mir, Moscow, 1984).
22. W. Hardle, *Applied Nonparametric Regression* (Cambridge Univ. Press, Cambridge, New York, New Rochell, Melbourne, Sydney, 1989; Mir, Moscow, 1993).

23. H. Hotelling, "Relations between Two Sets of Variates," Biometrika **28**, 321–377 (1936).

24. Y. Ida, M. Hayakawa, A. Adalev, and K. Gotoh, "Multifractal Analysis for the ULF Geomagnetic Data during the 1993 Guam Earthquake," Nonlinear Processes in Geophysics **12**, 157–162 (2005).

25. J. W. Kantelhardt, S. A. Zschiegner, E. Konsciently-Bunde, et al.,"Multifractal Detrended Fluctuation Analysis of Nonstationary Time Series," Physica A **316**, 87–114 (2002).

26. N. Kobayashi and K. Nishida, "Continuous Excitation of Planetary Free Oscillations by Atmospheric Disturbances," Nature **395**, 357–360 (1998).

27. D. Kurrle and R. Widmer-Schnidrig, "Spatiotemporal Features of the Earth's Background Oscillations Observed in Central Europe," Geophys. Res. Lett. **33**, L24304 (2006).

28. B. B. Mandelbrot, *The Fractal Geometry of Nature* (Freeman and Co., New York, 1982; Institute of Computer Investigations, Moscow, 2002).

29. S. L. Marple (Jr.), *Digital Spectral Analysis with Applications* (Prentice-Hall, Englewood Cliffs, New Jersey, 1987; Mir, Moscow, 1990).

30. A. N. Pavlov, O. V. Sosnovtseva, and E. Mosekilde, "Scaling Features of Multimode Motions in Coupled Chaotic Oscillators," Chaos, Solitons and Fractals **16**, 801–810 (2003).

31. C. R. Rao, *Linear Statistical Inference and Its Applications* (John Wiley and Sons, New York, London, Sydney, 1965; Nauka, Moscow, 1968).

32. A. Ramirez-Rojas, A. Muño-Diosdado, C. G. Pavia-Miller, and F. Angulo-Brown, "Spectral an Multifractal Study of Electroseismic Time Series Associated to the M_w = 6.5 Earthquake of 24 October 1993 in Mexico," Natural Hazards and Earth System Sciences **4** 703–709 (2004).

33. J. Rhie and B. Romanowicz, "Excitation Earth's Continuous Free Oscillations by Atmosphere–Ocean–Seafloor Coupling," Nature **431**, 552–554 (2004).

34. J. Rhie and B. Romanowicz, "A Study of the Relation between Ocean Storms and the Earth's hum-G_3: Geochemistry, Geophysics, Geosystems," Electronic "Earth Sciences" **7**(10.7) (2006); http://www.agu.org/journals/gc/.

35. L. Stehly, M. Campillo, and N. M. Shapiro, "A Study of the Seismic Noise from Its Long-Range Correlation Properties," J. Geophys. Res. **11**, B10306 (2006).

36. T. Tanimoto, J. Um, K. Nishida, and K. Kobayashi, "Earth's Continuous Oscillations Observed on Seismically Quiet Days," Geophys. Res. Lett. **25**, 1553–1556 (1998).

37. T. Tanimoto and J. Um, "Cause of Continuous Oscillations of the Earth," J. Geophys. Res. **104**(28), 723–739 (1999).

38. T. Tanimoto, "Continuous Free Oscillations: Atmosphere–Solid Earth Coupling–Annu. Rev.," Earth Planet. Sci. **29**, 563–584 (2001).

39. T. Tanimoto, "The Oceanic Excitation Hypothesis for the Continuous Oscillations of the Earth," Geophys. J. Int. **160**, 276–288 (2005).

40. L. Telesca, L. Colangelo, and V. Lapenna, "Multifractal Variability in Geoelectrical Signals and Correlations with Seismicity: a Study Case in Southern Italy," Natural Hazards and Earth System Sciences **5**, 673–677 (2005).

41. M. S. Taqqu, "Self-Similar Processes," in *Encyclopedia of Statistical Sciences*, Vol. 8, pp. 352–357 (John Wiley and Sons, New York, 1988).

42. A. R. Ziganshin and A. N. Pavlov, "Scaling Properties of Multimode Dynamics in Coupled Chaotic Oscillators—Physics and Control," in *Proceedings. 2005 International Conference*, pp. 180–183 (2005) [in Russian].